Mid–mantle anisotropy and mantle flow.

J–Michael Kendall[1], *James Wookey*[1] *and Guilhem Barruol*[2]

[1]*School of Earth Sciences, University of Leeds, England.*

[2]*Laboratoire de Tectonophysique, Université Montpellier, France.*

Introduction

Observations of mantle anisotropy are mainly confined to the uppermost and lowermost boundary layers (lithosphere and D'' region). There is though some evidence for anisotropy near what may be a boundary layer near the 660 km discontinuity [*Montagner and Kennett*, 1996; *Vinnik et al.*, 1998]). Here we present evidence for strong mid–mantle anisotropy in the vicinity of a subduction region. Our data suggest significant anisotropy just below the 660 km discontinuity.

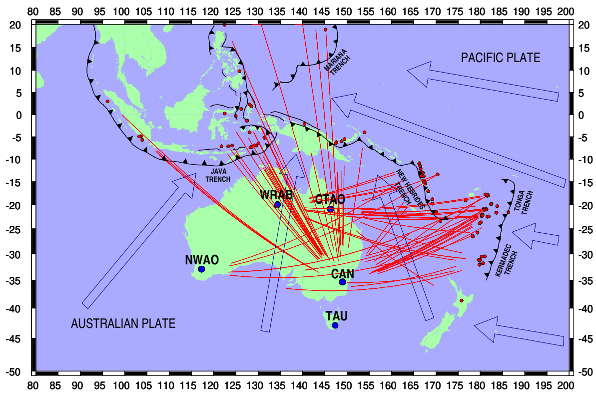

Figure 1. Dots show events and stations used to study mid–mantle anisotropy beneath Australasia. Lines show lower–mantle paths for each event–station pair and indicate the degree of azimuthal coverage. Also shown are subduction zones trenches and absolute plate motion directions.

Data

Earthquakes from the southwest Pacific subduction zones and recorded at stations in Australia are used to investigate the mid–mantle beneath Australasia [Figure 1]. Many of the Australian stations show little evidence of SKS splitting [e.g., CAN, *Barruol and Hoffman*, 1999] suggesting the upper–mantle beneath Australia is very weakly anisotropic, if at all. Such stations are therefore ideal observatories for studying source–side anisotropy. In contrast, S–phases which turn just below the 660 km discontinuity, 20^o to 40^o from the source, show very large amounts of shear–wave splitting (δt = 2–8 seconds) at these stations. These are some of the highest values of shear–wave splitting ever measured and suggest either very high degrees of localised anisotropy or wave propagation through a more moderately anisotropic region of large lateral extent.

We have made 290 splitting measurements, of which 102 give very convincing results (grade 1; $0.0 \leq \delta t \leq 0.5$ and $0 \leq \phi \leq 10$), 90 give reseasonable results (grade 2; $0.5 < \delta t \leq 1.0$ and $0 \leq \phi \leq 22$) and 98 give unreliable results (grade 3). Of the grade 1 results, 31 were from events >400 km deep. The polarisation of the fast shear–wave (ϕ) is predominantly horizontal [Figure 2] and, although the azimuthal coverage is somewhat limited [see Figure 1], thus suggests a transversely–isotropic symmetry.

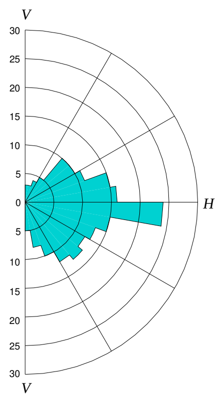

Figure 2. Rose diagram of the polarisation of the fast shear–wave (ϕ) obtained using the method of *Silver and Chan* [1988] for shear–wave splitting analysis. These results are for the grade 1 and 2 measurements only.

Modelling

To help guide interpretation of these observations we model waveform effects using anisotropic ray tracing and Maslov seismograms [*Kendall and Thomson*, 1993a, 1993b]. Models of anisotropy within the slab involve either a metastable olivine tongue which has a pre–existing anisotropy, or the preferred alignment of the akimotoite phase of enstatite which may exist under slab pressure and temperature conditions [*Anderson*, 1987]. Alternatively, the anisotropy may be due to crystal alignment near the 660 km discontinuity and not within the slab itself. It seems unlikely that the anisotropy could be explained by crystal alignment above 660 as ringwoodite is only mildly anisotropic. Below 660, the anisotropy could be due to the preferred alignment of perovskite, periclase or stishovite, all of which are highly anisotropic.

S–phases at these distances will be affected by the travel–time triplication due to the discontinuity at 660 km. We use Maslov theory to calculate the waveforms as ray theory waveforms will not be accurate near the cusps of the triplication. Unless the anisotropy is distributed uniformly across the discontinuity, each branch of the triplication will experience different degrees of splitting at a given distance. Such waveform effects will complicate the splitting analysis, so forward modelling is crucial in making any splitting interpretation at these distances.

The modelling also provides constraints on the degree of anisotropy in each model that is necessary to explain the observations [Figure 3]. It is almost impossible to explain more than 6 seconds of splitting in the deep focus events with anisotropy confined to the slab. The model with anisotropy beneath the 660 km discontinuity best explains the observations.

Conclusions

Observations of source–side shear–wave splitting combined with seismic modelling provide evidence for significant levels of anisotropy ($> 3\%$) in a boundary layer below the 660 km discontinuity in the vicinity of the Tonga–Kermadec and New Hebrides subduction zones. It is very unlikely that there are sufficient degrees of anisotropy within the subduction zones to produce the observed splitting. We speculate that the anisotropy is due to the preferred crystal alignment within a perovskite – periclase assemblage which is a result of lower–mantle deformation induced by the downwelling of the Tonga–Kermadec slab. Figure 4 shows a cap average of the anisotropy constrained to a 100 km thick layer at the top of the lower mantle.

It should be notes that SKS phases will not be affected by this mid–mantle transverse isotropy as they are vertically polarised at the core–mantle boundary and will not split in a transversely–isotropic medium. Furthermore, our models predict that ScS–phases will experience must less splitting than the sub–horizontally propagating S–phases due to their near–vertical propagation paths and short transit time through this region of mid–mantle anisotropy.

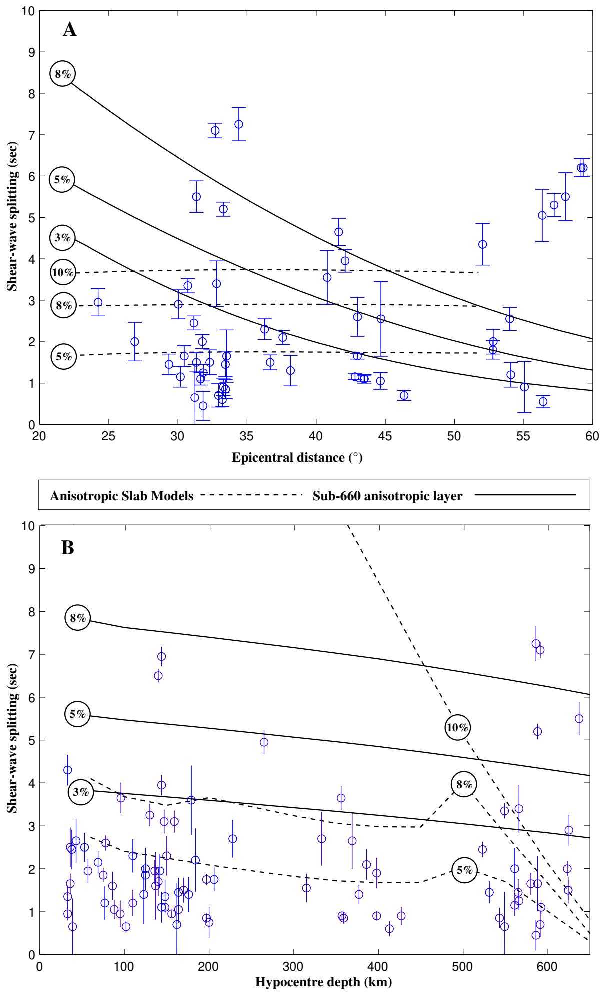

Figure 3. Comparison of data and modelling results. Dashed lines are for the anisotropic slab model and solid correspond to a model with a mid–mantle layer of anisotropy (percent values of anisotropy are indicated for each). (A) Splitting magnitude versus epicentral distance. The synthetic events have a fixed hypocentre depth of 550 km located inside the slab. The real data are the deep (hypocentre depth $>$ 400 km) Grade 1 and 2 data. (B) Splitting magnitude versus hypocentre depth. The synthetics are based on a fixed epicentral distance of 30^o. The real data are the Grade 1 and 2 results which fall in the distance range $25^o \rightarrow 35^o$.

References

Anderson, D. L., 1987, Thermally induced phase changes, lateral heterogeneity of the mantle, continental roots and deep slab anomalies, *J. Geophys. Res.*, *92*, 13968-13980.

Barruol, G. and R. Hoffmann, Upper mantle anisotropy beneath Geoscope stations, *J. Geophys. Res.*, *104*, 10757-10774, 1999.

Kendall, J-M. & C. J. Thomson, 1993a, Seismic modelling of subduction zones with inhomogeneity and anisotropy, I: Teleseismic P-wavefront geometry, *Geophysical Journal International*, *112*, 39-66.

Kendall, J-M. & C. J. Thomson, 1993b, Maslov ray-summation, pseudocaustics, Lagrangian equivalence and transient seismic waveforms, *Geophysical Journal International*, *113*, 186-214.

Montagner, J–P. and B. L. N. Kennett, How to reconcile body–wave and normal–mode reference Earth models, *Geophys. J. Int.*, *125*, 229-248, 1996.

Silver, P. G. and W. W. Chan, Implications for continental structure and evolution from seismic anisotropy, *Nature, 335*, 34-39, 1988.

Vinnik, L. P., S. Chevrot and J-P. Montagner, Seismic evidence of flow at the base of the upper mantle, *Geophys. Res. Lett.*, *25*, 1995-1998, 1998.

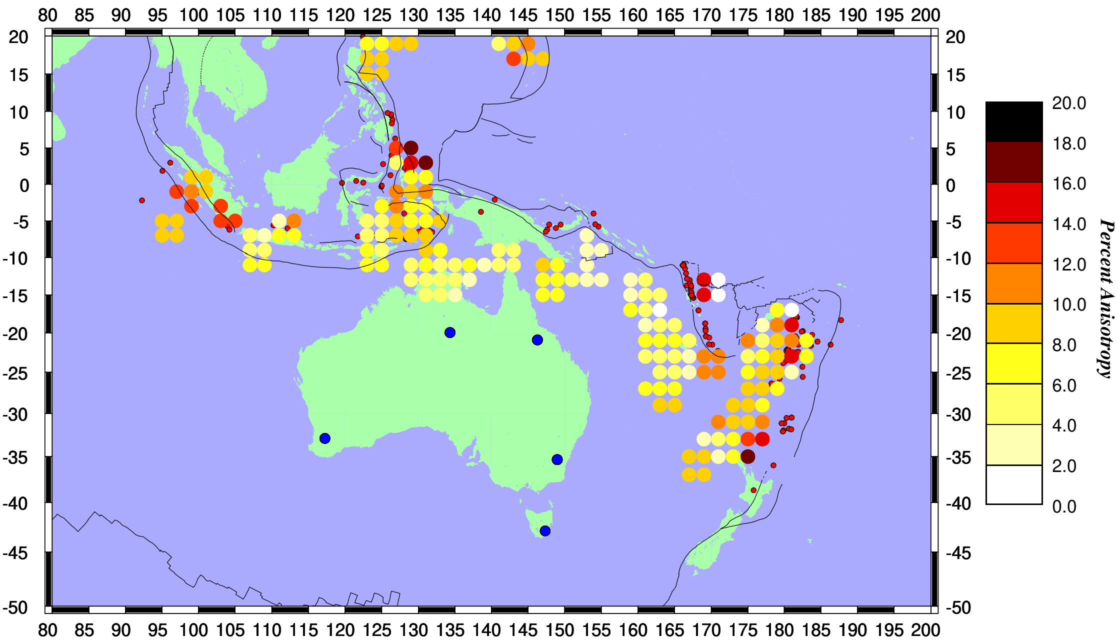

Figure 4. A cap–average of the magnitude of anisotropy required to produce the observed splitting. This assumes a 100 km thick layer at the top of the lower mantle. Cap size is 2^o and the results are plotted at the source–side point where the S–phase enters the lower mantle.